Clinical Chemistry 44:9
2036–2043 (1998)

Oak Ridge Conference

Mass-sensing, multianalyte microarray immunoassay with imaging detection

John W. Silzel,* Bibijana Cercek,[1] Charles Dodson, Tsong Tsay, and Robert J. Obremski

Miniaturization of ligand binding assays may reduce costs by decreasing reagent consumption, but it is less apparent that miniaturized assays can simultaneously exceed the sensitivity of macroscopic techniques by analyte "harvesting" to exploit the total analyte mass available in a sample. Capture reagents (avidin or antibodies) immobilized in 200-μm diameter zones are shown to substantially deplete analyte from a liquid sample during a 1–3-h incubation, and the assays that result sense the total analyte mass in a sample rather than its concentration. Detection of as few as 10^5 molecules of analyte per zone is possible by fluorescence imaging in situ on the solid phase using a near-infrared dye label. Single and multianalyte mass-sensing sandwich array assays of the IgG subclasses show the sensitivity and specificity of ELISA methods but use less than 1/100 the capture antibody required by the 96-well plate format.

Reduction of size appears to offer many anticipated advantages such as reduced costs, faster chemistry, and equivalent or perhaps improved sensitivity. Our area of interest is ligand binding assays in which the analyte is quantified, directly or indirectly, on the basis of its specific affinity for a chemically modified solid material. This broad class includes hybridization assays for specific DNA sequences, immunoassays using immobilized antigen or antibody, and the receptor assays used in high throughput screening of pharmaceuticals. In addition to the benefits noted above, we will demonstrate a multianalyte capability with all analytes exposed to the solid phase simultaneously and measured simultaneously.

Our efforts in "scaling down" assay technologies began in 1993 and arose out of a desire to maximize the useful analytical signal from any given assay system. Specifically, our experiments indicated that direct laser-induced fluorescence detection afforded greater dynamic range and simplicity than many assay detection methods involving enzyme amplification. Background fluorescence from biologicals, which often limits the sensitivity of direct fluorescence in the visible region, was largely circumvented in our laboratory by the use of fluorophores absorbing and emitting in the short wave near-infrared region (NIR), where biologicals are more optically inert *(1)*. Sensitivity using laser-induced fluorescence in the NIR was then limited principally by Raman scattering from the solvent (generally water) and by the optical considerations of achieving efficient excitation of a solution volume or solid phase having dimensions on the order of 0.5–1 cm.

A solution to these problems was envisioned in the placement of the entire solid phase "sorbent" for an assay in a microscopic volume, which could be efficiently probed by simple laser optics. Removing the solid phase from the liquid environment and making our measurements in the absence of liquid would then eliminate solvent backgrounds. We anticipated, as have Ekins et al. *(2–4)*, that the background fluorescence or scattering related to the solid phase itself would fall off as the viewed sorbent area was reduced. However, our use of the NIR largely reduces this background to the inevitable Raman scattering, and our overriding concern was the maximization of signal. To achieve this maximization, we have developed methods for preparing microscopic sorbent zones in an effort to maximally perturb the sample concentration by harvesting the entire analyte mass, to the extent possible, onto the microscopic measurement region. In our assay regime, therefore, the microscopic sorbent region acts as a sample concentration device. Unlike the "ambient analyte" regime of Ekins et al. (*2*, *3*) that measures analyte concentration, our method detects instead the analyte mass present in the applied liquid volume. In theory, this mass assay regime would yield an equivalent response to a 100-μL sample containing 10^{-13} mol/L analyte or a 10-μL aliquot containing the same analyte at 10^{-12} mol/L. This presupposes equilibration of

Beckman Coulter, Inc., 200 South Kraemer Boulevard, Brea, CA 92822-8000.
[1] Present address: 4318 Camphor Avenue, Yorba Linda, CA 92886.
* Author for correspondence. Fax 714-993-8639; e-mail jsilzel@beckman.com.
Received May 6, 1998; revision accepted June 15, 1998.

the capture reagent with the liquid bulk, which will be addressed in *Materials and Methods*.

MASS ASSAY THEORY

Consider a thyroid-stimulating hormone assay performed using the proposed "mass assay" method. Our typical binding capacity in a single 200-μm sorbent zone is on the order of 10^{10} analyte molecules (see *Materials and Methods*). If this zone were in contact with a 100-μL sample volume, the effective "concentration" of sorbent would be 1.7×10^{-10} mol/L. Note that this is 1–2 decades higher than the 0.01 K^{-1} dictated by "ambient analyte" theory, because most optimized antibodies have K near 10^9 or 10^{10}.

$$K = \frac{xVN}{(Ab_o - x) \cdot (Ag_o - x)} \quad (1)$$

Eq. 1 describes x, the number of molecules of antigen-antibody complex present in a system of volume V at equilibrium, assuming an affinity constant K, with Ab_o and Ag_o moles of antibody and antigen, respectively, present initially. The quantity N is Avogadro's number. Under ambient analyte conditions, the complex would have little effect on the concentration in solution, and the variable x can be dropped in the terms of the denominator. Assuming $K = 10^{10}$ liter mole^{-1}, a volume of 100 μL, and 60 000 molecules of thyroid-stimulating hormone available for assay (10^{-15} mole liter^{-1}), 600 molecules would be bound and provide signal. In the mass assay method, Eq. 1 must be solved in the more general quadratic form, which takes into account the effect of x on the denominator. This calculation predicts that at equilibrium, roughly 38 000 molecules of analyte are bound, >60% of the total analyte mass available. The absolute fluorescence signal expected from the mass assay is 60 times that calculated from the guidelines proposed for ambient analyte conditions. The theoretical advantage in percent recovery is maintained at higher analyte concentrations, as indicated by comparison of the solid (mass assay) and dashed (ambient analyte) lines computed in Fig. 1.

Of course, these models and discussion are predicated on the assumption that chemical equilibrium can be reached in microscopic-scale ligand binding assays under reasonable conditions. The formulation of thermodynamic chemical activities in Eq. 1 using the total liquid volume clearly ignores the kinetic diffusive barrier between the bulk solution and a microscopic sorbent region, which must operate in any real system *(5)*. Certainly the mass assay method calls for the minimization of the assay volume (by the avoidance of sample dilution) to facilitate maximum harvest of analyte. The experiments described in this report focus on determining the practical feasibility of the mass assay methods using a simplified ligand binding system (avidin and biotin) and the extension of the mass sensing microarray format to single analyte immunoassay of human IgG. Finally, a multianalyte array assay of the four human IgG subclasses is demonstrated.

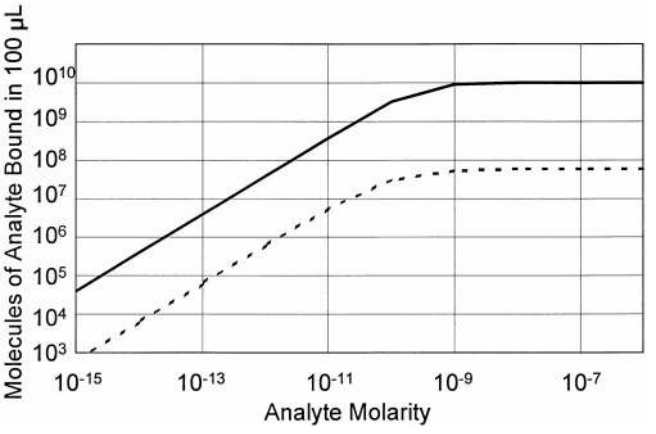

Fig. 1. Computed hypothetical thyroid-stimulating hormone assay equilibria for "mass assay" (——) and "ambient analyte assay" (- - - -) regimes.

An antibody affinity of 10^{-10} liter mole^{-1} and a volume of 100 μL are assumed. Mass assay assumes 10^{10} binding sites per 100 μL.

Materials and Methods

The highly specific binding of biotin by the protein avidin was selected as an optimal ligand binding assay model with binding affinity about 10^{15} liter mole^{-1}. For this work, a deglycosylated commercial avidin preparation (NeutrAvidin, Pierce Chemical Co.) was used, although no statistically significant differences in binding capacity, background, or sensitivity were observed when ordinary streptavidin or avidin were substituted.

The fluorescent NIR dye chosen for this work, DBCY5, is the dicarbocyanine analog of indocyanine green, synthesized in-house. The dye was biotinylated by reaction of its *N*-hydroxysuccinimidyl ester derivative, in excess, with biotin hydrazide. The resulting biotin derivative has an absorbance maximum near 670 nm, with fluorescence emission occurring at 710 nm. The molar absorptivity in aqueous solutions is 200 000, and the quantum efficiency is ~20%. These spectral properties are essentially unchanged from the unconjugated dye. Assessment of the degree of biotinylation was performed by two methods. The first involved incubating a single aliquot of the product successively in several wells of a commercially prepared avidin-coated microtiter plate (Pierce Chemical Co.) and noting the residual fluorescence of the solution after removal of all biotinylated material. In this manner, it was determined that 70% of the NIR dye molecules in the product were biotinylated. A second procedure involved the conventional assay of biotin *(6)* using 4-hydroxyazobenzene-2-carboxylic acid (Pierce Chemical Co.) to confirm the absence of unlabeled biotin residues that would reduce sensitivity by blocking avidin sites.

Microscopic reagent zones were prepared by loading the desired reagent solution into a previously disassembled and ultrasonically cleaned printhead unit of a desk-

top jet printer (Hewlett Packard ThinkJet). A 3″ × 3″ sheet of precleaned polystyrene film (Whatman Inc.) having a 250-μm (1 mil) thickness was taped to tractor paper and loaded into the printer. Film was precleaned by rinsing in absolute methanol and drying, using an inert gas duster of the type commonly sold for photographic use (Kensington Microware, Ltd.). The volume dispensed on each activation of a printer jet was determined by printing a predetermined number of droplets of DBCY5 dye solution of known concentration onto film, then rinsing the dye from the film with a known volume of methanol. The fluorescence of the wash solution was then compared with calibrator solutions of DBCY5 in methanol. By using this method, the mean droplet volume was determined to be 80 pL.

The experimental apparatus used to measure fluorescence from the printed zones is shown in Fig. 2. Briefly, imaging detection of fluorescence from the microscopic zones was done using a Peltier cooled charge coupled device camera (Princeton Instruments, Inc.) coupled to a ×6.5 microscope objective (Melles Griot) and appropriate excitation and emission filters (Omega Optical filter set XF-48) to detect isotropic emissions from the film. Evanescent wave excitation of fluorescence from the printed zones was realized by launching filtered emissions at 670 nm from a GaAlAs diode laser (Lasiris, Inc.) into the film using a prism coupler of our own design. Quantitative analysis of the resulting 16-bit image data was performed using an automated macro driving the intrinsic functions available in a commercial software package (ImagePro 3.0, Media Cybernetics, Inc.).

An assessment of the sensitivity and reproducibility of the printing and measurement processes was made by printing calibrator solutions of native DBCY5 dye, then constructing dose–response curves from the reduced image data. As shown by Fig. 3, the imaging system has a mass detection limit of $\sim 10^5$ DBCY5 molecules per printed zone. Volumetric precision of the inkjet printer is

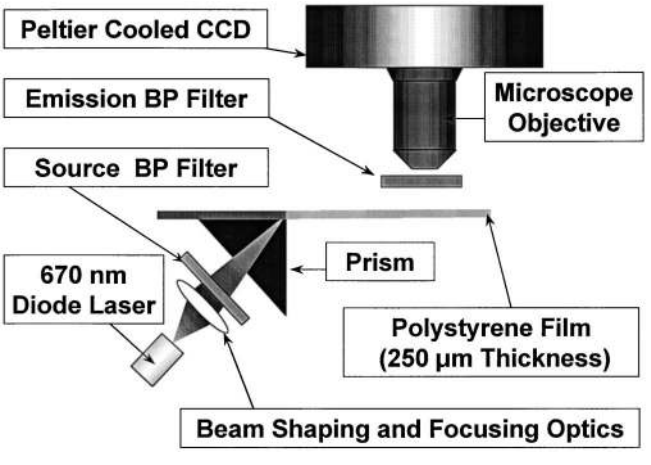

Fig. 2. Schematic diagram of experimental apparatus for the evanescent wave excitation and fluorescence imaging detection of microarrays printed on flexible polystyrene film.

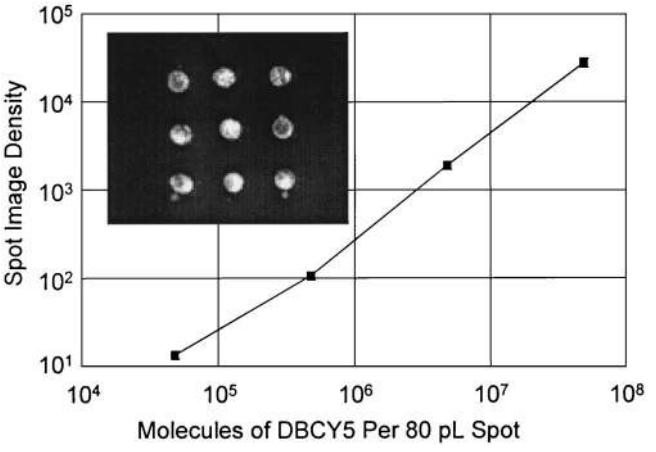

Fig. 3. Imaging detection of DBCY5 dye printed using solutions of known concentration allows determination of precision and detection limits.

Inset shows a typical charge coupled device image of a microarray.

such that 1 SD about the mean of spot intensities in a nine-spot array is ~6%. The limit of detection is imposed by a background that is a combination of residual, spurious, long wavelength emissions from the diode laser and Raman scattering from the polystyrene film.

Arrays of immobilized avidin spots were prepared by printing a solution of 1 g/L NeutrAvidin in buffered solution. This concentration is higher than what is typically used for the coating of microtiter plate wells but is understandable on the basis of the very different volume-to-surface area characteristics presented by the microscopic experimental scale. The printed spots dry within 30 s of deposition, leaving a visible solid residue that permits visible examination of the array and gross verification of printer function. For noncovalent immobilization, a 50 mmol/L carbonate buffer at pH 8.2 was used for printing. For covalent immobilization, the buffer was 50 mmol/L phosphate-buffered saline at pH 7.4. Covalent immobilization was achieved by derivatization of NeutrAvidin with a commercial photolabile linker moiety. After printing of this NeutrAvidin-linker conjugate, covalent immobilization was obtained by exposing the dry printed arrays to light from a UV source (Dymax 2000EC) for 3 min. Subsequent experience with dry avidin arrays has indicated that these materials are stable under refrigerated vacuum desiccation for at least 6 months.

Immediately before use, printed arrays were washed to remove any loosely bound avidin. This washing was accomplished with PBS/T, a 2 mL/L solution of Tween 20 in phosphate-buffered saline, pH 7.4. Assay of biotin-DBCY5 was then performed by incubating printed arrays with various volumes and concentrations of DBCY5-biotin conjugate diluted in PBS/T. Incubation times were varied from 30 min to 24 h, using a microtiter plate shaker (Lab Line, Inc.) or rotating wheel (Glas-Col), depending on the sample volume under study. After the incubation, the PBS/T wash was repeated to remove free DBCY5

and/or loosely bound DBCY5-biotin. A final rinse in deionized water was performed to remove buffer salts from the film before drying. The arrays were then dried using an inert gas duster (Kensington Microware, Ltd.) and imaged within 1 h.

Immunoassay of the human IgG subclasses was performed using biotinylated monoclonal antibodies (clones HP-6091, HP-6014, HP-6050, HP6025, and HP-6047, Sigma Chemical Co.) by a protocol derived from that of Hamilton et al. *(7)*. Antibody arrays were generated either by incubation of avidin printed arrays with an excess of biotinylated capture antibody or by direct jet printing of antibody to form multianalyte arrays. The arrays were then washed and blocked with a 5 g/L solution of bovine serum albumin in PBS and incubated for 30 min to 24 h with 50 μL of solution containing human myeloma proteins (Sigma Chemical Co.) diluted in 1 g/L bovine serum albumin. Arrays were then washed and incubated for 1 h with polyclonal mouse anti-human IgG (Jackson Immunoresearch) labeled with ~2.8 DBCY5 molecules per antibody. Finally, the arrays were washed, dried, and imaged as done in the avidin/biotin system.

Results and Discussion

Fig. 4A shows typical dose–response curve results obtained by titration of nine-spot avidin arrays with four different fixed volumes of DBCY5-biotin solution prepared by serial dilution. The mean charge coupled device pixel intensity computed from the imaged fluorescent spots tracks dye-biotin concentration in the quantitative manner expected from conventional binding assays. The data in Fig. 4A reflect 1 h incubation time; although signal was observed to increase with incubation times from 30 min to 3 h, signals after 15 h of incubation were found to be only slightly higher than after 3 h. Sensitivity did not improve past 1 h of incubation time. A standard incubation time of 1 h was adopted in the avidin-biotin work.

In the mass sensing microassay format, maximization of signal is achieved by maximizing the functional analyte binding capacity per unit area. Dose–response curves from noncovalently immobilized avidin arrays exhibit a relatively low density of binding sites relative to covalent attachment (Fig. 4A). Noncovalent immobilization was also found to be susceptible to desorption and loss of capture reagent during wash steps with surfactant (2 mL/L Tween 20) present. These results have led to the abandonment of noncovalent attachment in favor of covalent immobilization methods. By using covalent immobilization, signal losses in wash steps have been found to be unimportant, and we believe that retention of bound analyte on the printed arrays is facilitated by the high local concentration of binding sites experienced by bound species *(8, 9)*.

Atomic force microscopy (AFM) of an immobilized avidin spot after washing indicates that the covalent printed array spots have an irregular topology extending up to 200 nm vertically from the surface of the film.

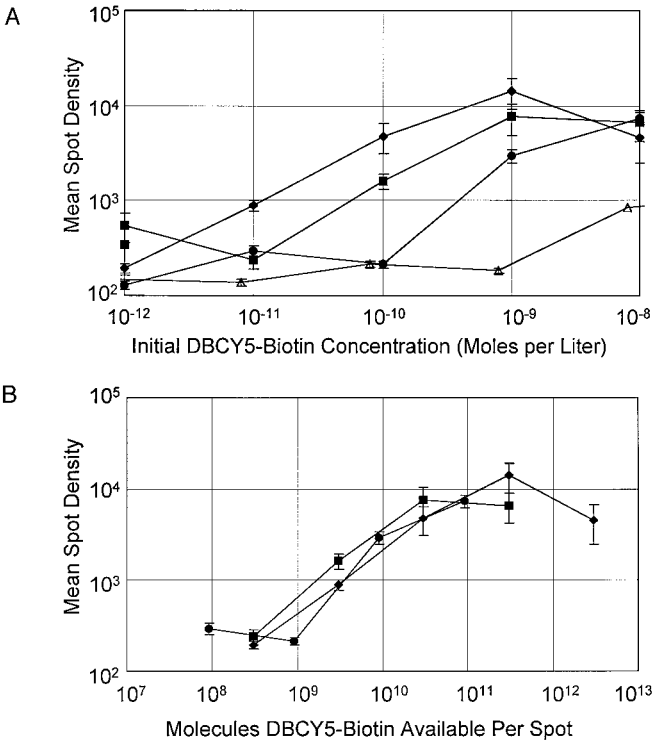

Fig. 4. DBCY5-biotin dose response.

(*A*) Dose–response data for DBCY5-biotin incubated with printed avidin microarrays. Data show dependence on the volume of the sample, which was varied from 5 mL (♦) to 500 μL (■) to 150 μL (●). Noncovalent adsorption of avidin to polystyrene film yields low signals (△). (*B*) When the data from *A* for 5 mL (♦), 500 μL (■), and 150 μL (●) sample volumes are plotted vs DBCY5-biotin mass present, the dependence of signal on analyte mass, rather than concentration, is apparent. This result indicates that analyte "harvesting" is taking place.

Integration of the AFM topology data indicates that the dry residue composing one "spot" has a volume on the order of 6×10^{-11} cm^3, placing an upper limit on the mass of avidin of roughly 190 pg/spot, assuming each avidin molecule occupies 6 nm^3 in the dry matrix *(10)*. Because ~100 pg of avidin was deposited per spot in the AFM study (100 pL of 1 g/L solution), the AFM experiments indicate that most of the avidin mass actually printed is covalently incorporated into the spot "structure". The printed avidin spots in the AFM study were titrated with DBCY5-biotin solutions of known concentration and found to have a binding capacity on the order of 10^9 dye-biotin molecules per spot, equivalent to roughly 100 pg of avidin per spot, assuming one binding site per avidin molecule. This result, together with the AFM data, implies that between one and two active sites are present per avidin molecule after printing and immobilization. (Note that the signal levels in Fig. 3 result from higher laser power and cannot be used to quantify binding capacity by comparison with Fig. 4.)

If the printed volume is increased from 100 pL to 1 nL, the spot diameter roughly doubles to 200 μm. Titration of these larger spots with DBCY5-biotin then indicates a functional binding capacity on the order of 10^{10} dye-biotin molecules bound per printed spot, or roughly 3500

ng/cm^2, assuming one binding site active per avidin molecule. This binding site density is roughly 20 times higher than the 130–150 ng/cm^2 typically specified for commercial avidin-coated polystyrene microtiter plates, probably because of the complex topology of the printed spots.

The titration curves obtained from these 200-μm spots show dependence on the volume of the dye-biotin solution present during the 1 h incubation (Fig. 4A). As the volume of dye solution in contact with the arrays is increased from 150 μL to 500 μL to 5 mL, the titration curve appears to shift to the left along the dye-biotin concentration axis, toward lower concentrations. This effect results from the larger number of dye-biotin molecules available to the printed spots, at any one concentration, as the volume of the "sample" is increased. If the same data are plotted as a function of the total analyte mass present, rather than concentration, the data for all three volumes are found to agree to within the SD about the mean pixel image intensity of the nine spots in each array (Fig. 4B). The printed avidin arrays respond to analyte mass, not to concentration, because they have sufficient affinity and binding capacity to markedly deplete the solution of dye-biotin, without regard to the sample volume, under the experimental conditions. The functional detection limit for DBCY5-biotin can be arbitrarily defined as the dye-biotin concentration that yields a mean spot fluorescence intensity in a nine-spot array at least 3 SDs above the mean of a "blank" array incubated for 3 h with standard PBS/T solution. In the standard 1-h incubation, this functional detection limit is encountered when the initial dye-biotin solution provides a mass on the order of 10^6 molecules of dye-biotin per spot (Fig. 5). As in the dye printing experiment (Fig. 3), the sensitivity limitation is imposed by the spectroscopic background characteristic of the instrumentation used.

If the number of avidin spots is varied in a mass-sensing array, the law of mass action would imply that the density of analyte bound per spot should vary inversely with the number of spots present. When fewer spots are printed per array, the total analyte mass present during incubation is collected onto fewer spots, leading to increased signal from any one spot. Fig. 6 shows experimental results from 3-h incubations in which 100-μL aliquots of 10^{-11} mol/L DBCY5-biotin solution were in contact with arrays having 1, 9, 25, 49, or 70 spots. Also shown on the plot is the signal predicted by quadratic solution of the mass action law, assuming an affinity constant for avidin of 10^{15} mol/L^{-1}, a binding capacity of 10^{10} biotin-dye molecules per spot, and a mean fluorescence image intensity of 10^4 at binding site saturation (compare Fig. 4B). The experiment confirms the mass-sensitive nature of the avidin arrays and also indicates that the 3-h incubation gives results comparable with those expected based on thermodynamic considerations alone. Microscopic diffusive transport of biotin-DBCY5 from bulk solution to the printed spots is apparently rapid enough for practical microarray assays to operate in a mass-sensing regime while using conventional incubation times on the order of 1-3 h.

ASSAY OF HUMAN IgG3

The avidin-biotin system described was extended to the assay of human IgG3 by incubation of standard printed avidin arrays with an excess of biotinylated HP-6050 monoclonal antibody specific for the IgG3 subclass, using the assay protocol described in *Materials and Methods*. Fig. 7 shows dose–response curves resulting from assay of 50-μL aliquots of human myeloma proteins (kappa chain). Subclass-specific response to IgG3 was observed, based on negative control experiments using solutions of human myeloma proteins of different subclasses (an IgG4-negative control is shown in Fig. 7). Fig. 7 indicates that a 24-h sample incubation yields insignificant signal gains over a 2-h incubation. Use of a 1-h incubation (not shown) gives

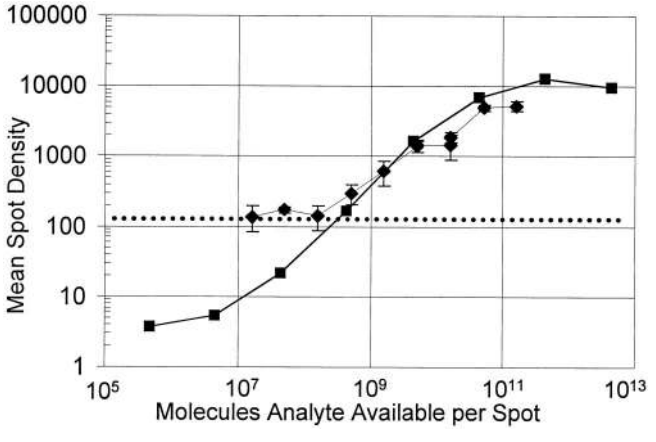

Fig. 5. Dose–response characteristics of the IgG3 assay (♦, 2-h incubation) and avidin-biotin system (■, 1-h incubation), plotted against mass units.

The nonspecific binding amount (····) limits the immunoassay sensitivity, but maximum signals are comparable in the two systems.

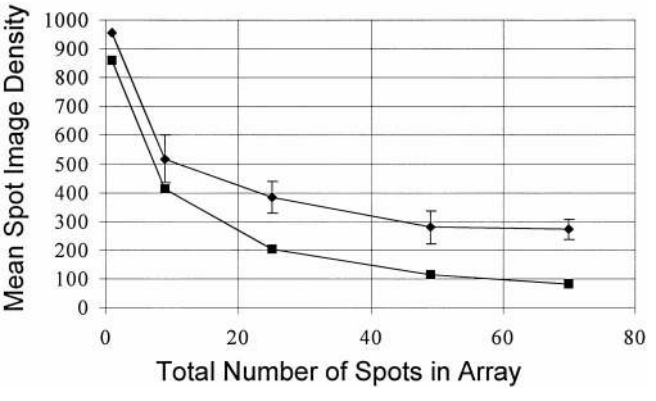

Fig. 6. Reducing the number of spots per array while holding the dye-biotin concentration constant at 10^{-11} mol/L (♦) gives increasing signal and further evidence of harvesting.

Comparison with an equilibrium model (■) indicates that marked "harvesting" is not precluded by kinetic limitations.

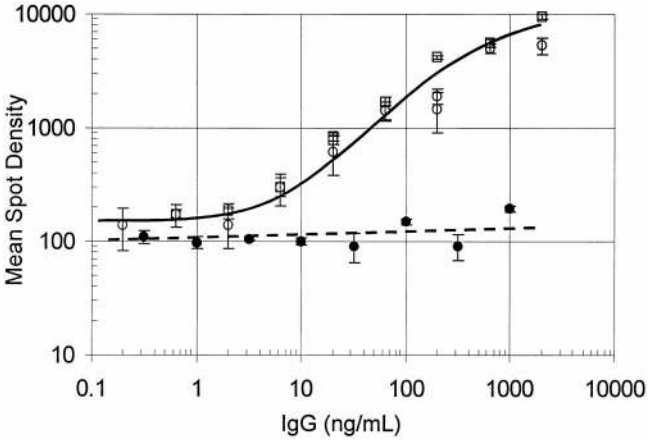

Fig. 7. Dose–response curves for IgG3 microarray assay using sample incubation times of 2 h (○) and 24 h (□).

Specificity is observed for the IgG3 subclass relative to a control experiment (2-h incubation) with IgG4-class myeloma (●). A 1-h incubation yields the same signals at IgG3 concentrations below 100 μg/L but falls off to a maximum signal of 3000 at the highest IgG3 concentrations.

the same amount of sensitivity but a decrease in maximum signal. Although the performance of the 1-h incubation would be tolerable in a practical assay, a standard 2-h incubation was adopted arbitrarily. The detection limit for IgG3 (arbitrarily defined as the interpolated IgG concentration at which image density of the spots in the array is 3 SDs greater than a blank experiment) was ~15 μg/L, a concentration providing about 3×10^8 molecules of IgG3 per array spot. A conventional ELISA plate assay *(7)* has been reported to have a sensitivity of 2 μg/L, using a monoclonal antibody having an 8-fold higher affinity *(7)* for IgG3 (clone HP-6047). On the basis of equilibrium considerations, a microarray IgG3 assay using the higher affinity antibody should demonstrate sensitivity comparable with the ELISA, despite the use of direct fluorescence. We attribute this amount of sensitivity to the harvesting of analyte mass from bulk solution, concentrating the analyte on the printed spots to a degree that removes the need for an enzyme/substrate amplification system and permits use of the simpler direct fluorescence labeling. The limit of detection in the IgG3 assay is imposed by immunochemical nonspecific binding, which is observed to occur only to the printed spots rather than the blocked, untreated polystyrene areas between the arrays. The nonspecific binding background signal is ~100 times the instrumental detection limit observed for the avidin-biotin system (Fig. 5), implying that the microarray technique is capable of detecting 10^6 molecules/spot if the nonspecific binding were to be reduced to the amount encountered in the avidin-biotin system.

The maximum signals observed in the IgG3 dose–response data are comparable with those measured in the dye-biotin system (Fig. 5). Apparently any steric constraints that limit the access of antibody reagents to the avidin binding sites are offset by the use of multiple fluorescent labels on the polyclonal probe antibody. The IgG3 and avidin/biotin dose–response data also have similar shape when plotted vs total number of analyte

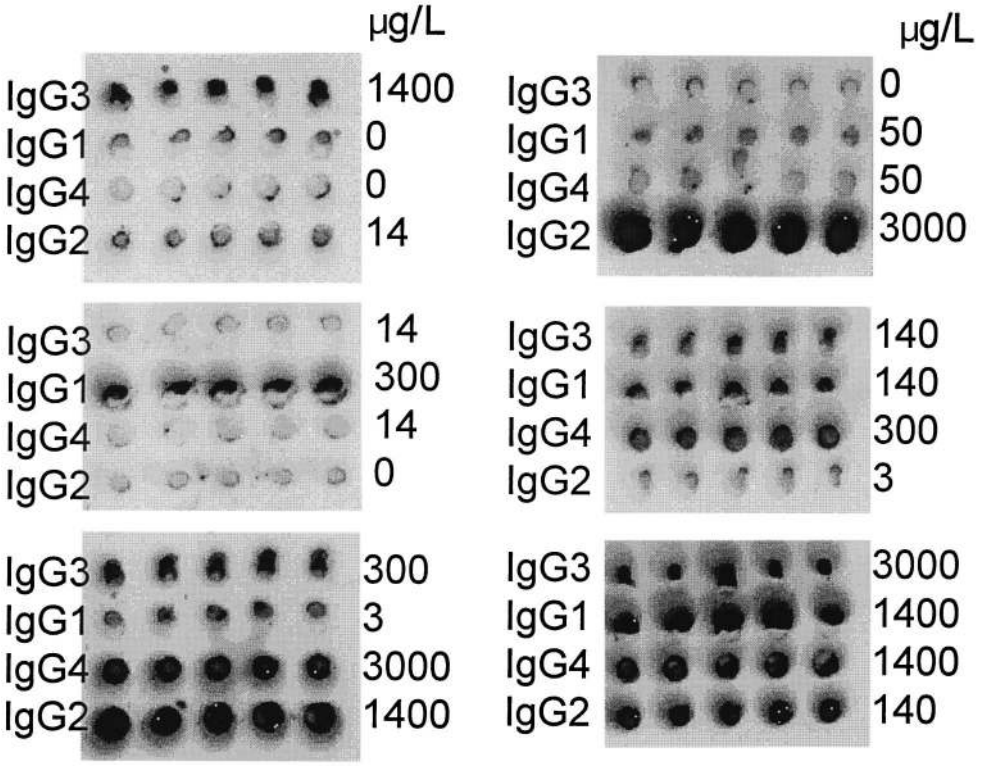

Fig. 8. Raw image data from the four-analyte human IgG subclass assay.

Numbers beside each microarray row indicate the expected concentration of each subclass in the four-component myeloma mixture assayed in a given image.

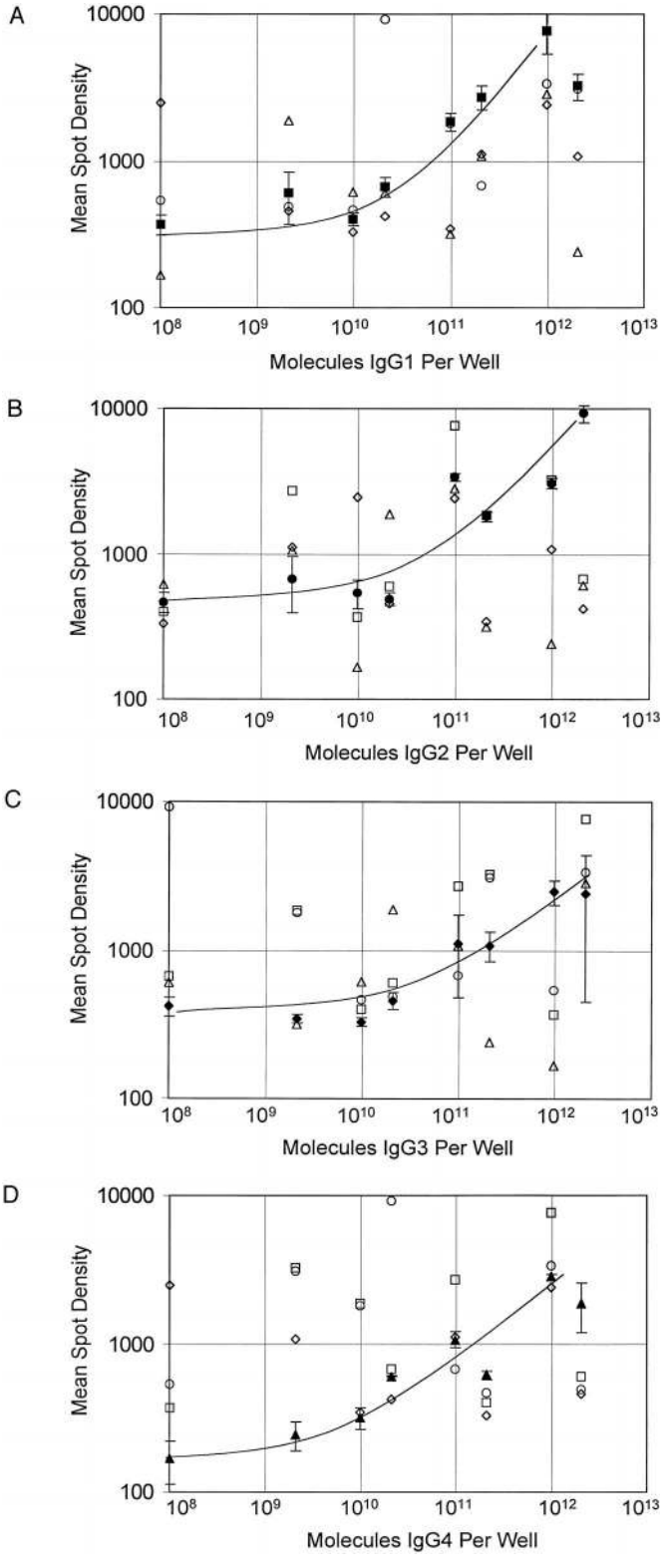

Fig. 9. (*A–D*) Signals from the IgG1 (■)-, IgG2 (●)-, IgG3 (♦)-, and IgG4 (▲)-specific spots in each image are plotted vs the expected myeloma concentrations in the corresponding well.

(●) Fluorescence from subclass-specific microarray spots that "match" the subclass plotted on the *x*-axis. (○) Spots not specific for the plotted myeloma subclass.

molecules per well, neglecting the nonspecific binding amount of the assay. This agreement is consistent with the operation of the immunoassay in the mass-sensing regime, despite the reduced affinity of the assay (10^8 liter $mole^{-1}$)as compared with the avidin/biotin system.

MULTIANALYTE IMMUNOASSAY OF THE FOUR HUMAN IgG SUBCLASSES

Extension of the IgG3 assay to a multianalyte array assay of all four human IgG subclasses was performed by jet printing of a 1 g/L monoclonal antibody solution to form arrays in which each row of 200-μm spots recognize a different IgG subclass. Each spot was generated using 1 nL of solution. Eight different mixtures of human myeloma proteins from each subclass were prepared in PBS solution with 5 g/L bovine serum albumin and assayed using the same protocol developed for assay of IgG3 (2-h incubation). The mixtures assayed included pseudo-random combinations of myeloma concentrations between 10 mg/L and 10 μg/L, as well as mixtures in which one subclass was not present. After the sample incubation and washing, the DBCY5-labeled polyclonal mouse anti-human IgG reagent was then used to develop signals from all four assays simultaneously. The image data for the four-analyte array (Fig. 8) show qualitative dependence between spot intensity along each row and the expected concentration of the appropriate myeloma subclass in the 50-μL IgG mixture aliquots assayed. (Note that Fig. 8 is a "negative image" in which the brightest image areas appear dark in the figure.) Quantitative image processing of the multianalyte data yields the results shown in Fig. 9. For each IgG subclass, the mean spot fluorescence density computed across each array row is plotted against the myeloma protein concentration in the mixtures. Data from spots specific for the appropriate IgG subclass concentration ("filled" points) show the expected dose–response dependence of signal on myeloma concentration. Detection limits may be crudely estimated from these dose–response data and appear to be similar to the 15 μg/L observed in the single-component IgG3 assay.

Evidence for subclass specificity is seen in the lack of systematic correlation between myeloma concentration and measured fluorescence image density observed in the "open" points plotted in Fig. 9. These points show data from microarray rows plotted vs myeloma concentrations for the incorrect (nonmatching) subclasses. Multilinear regression on the multianalyte array data indicates that any cross-reactivity between the assays is sufficiently small as to be obscured by the spot-to-spot variability within the columns. This error is currently 10–15% of the mean intensity in one row (1 SD) owing to mechanical difficulties encountered in the jet printing of multiple antibodies. The low amount of cross-reactivity indicates that antibody specificity can be retained despite the rigors of jet printing and drying. Stability of dry-printed multianalyte arrays has been shown to be dependent on the particular antibodies immobilized but has been demon-

strated to exceed 1 month if arrays are stored in a refrigerated vacuum desiccator and coated with a commercial immunoassay stabilizer preparation (StableCoat, SurModics, Inc.).

That this multianalyte array assay senses the available mass of each analyte rather than its concentration can be shown by preparation of microarrays containing spots specific for IgG3 and IgG4, with some arrays also containing a third monoclonal recognizing both IgG3 and IgG4 (clone HP6017). These experiments demonstrate intraarray competition, with the IgG3 and IgG4 signals being reduced, relative to controls, in the presence of the spots recognizing "total" IgG. This effect would not be seen if the sample solution in contact with the array were not being depleted of analyte and confirms that signals in the multianalyte array assay are being enhanced by "harvesting" and concentration of the analyte on the printed spots. Intraarray competition must be taken into account in mass-sensing multianalyte arrays designed to sense total IgG in addition to the subclasses.

Although the mass-sensing microarray assay format provides a high density of binding sites, the extremely small scales involved lead to an overall decrease in the mass of antibody required per test. Approximately 1 ng of antibody is deposited per spot in the printed arrays, compared with the 100 ng typically immobilized in one well of a 96-well microtiter plate. The actual savings in reagent may be even greater than this because as much as 200–300 ng of antibody are often added per well during (noncovalent) plate coating to yield a "securely" bound antibody mass of 100 ng/well. This potential cost savings may be important in many applications.

Jet-printed spots of reagent having diameters of 100–200 μm can be prepared using solutions of avidin or antibodies that retain specificity and affinity for their targets. When binding site density is maximized and binding sites are present in excess, the spots can effectively deplete analyte from bulk solution to yield high local analyte concentration on the printed spot. This harvesting of analytes maximizes signal to background ratios and permits the detection of 10^5 or fewer analyte molecules by direct fluorescent labeling, without resort to enzyme amplification. In this regime, the detected signal depends on the total analyte mass in a sample, rather than its concentration. Once analyte molecules are bound by the microarray, they are quite resistant to loss during wash steps. A simple immunoassay of IgG3 using the mass-sensing microarray approach has demonstrated sensitivity equal to a conventional ELISA plate assay and has been extended to a simultaneous multianalyte assay of the four human IgG subclasses in a single 50-μL sample aliquot. Detection limits of the microarray assay are consistent with the published sensitivity of conventional plate assays using similar immunoreagents and protocols, despite the fact that the microarray approach requires less than 1/100 the antibody mass of conventional microtiter plate assays using coated wells.

We thank Robert C. Dunn of the Chemistry Department at the University of Kansas for providing AFM data for the printed spots; we also thank David Wallace, Paul Watson, and Patrick Cooley at MicroFab, Inc. for jet printing of microarray materials; Gene Shen at Beckman Coulter for synthesis of the near infrared fluorescent dye and its conjugates; and Tom Stachelek of Beckman Coulter for experimental work leading to design of the prism coupler apparatus.

References

1. Obremski RJ, Silzel JW, Tsay TT. Near IR fluorescence: instrumentation, application, and pitfalls. In: Burgess C, Jones DG, eds. Spectrophotometry, luminescence and colour: science and compliance. Amsterdam: Elsevier, 1995:235–46.
2. Ekins RP, Chu FW. Multianalyte microspot immunoassay–microanalytical "compact disk" of the future. Clin Chem 1991;37:1955–67.
3. Ekins R, Chu F, Biggart E. Development of microspot multi-analyte ratiometric immunoassay using dual fluorescent-labelled antibodies. Anal Chim Acta 1989;227:73–96.
4. Ekins R, Chu F. Multianalyte testing [Letter]. Clin Chem 1993;39:369–70.
5. Nygren H, Stenberg M. Kinetics of antibody-binding to surface-immobilized antigen: influence of mass transport on the enzyme-linked immunosorbent assay (ELISA). J Colloid Interface Sci 1985;107:560–6.
6. Green NM. A spectrometric assay for avidin and biotin based on binding of dyes by avidin [Short Communication]. Biochem J 1965;94:23C.
7. Hamilton RG, Wilson RW, Spillman T, Roebber M. Monoclonal antibody-based immunoenzymetric assays for quantification of human IgG and its four subclasses. J Immunoass 1988;9:275–96.
8. Stenberg M, Nygren H. Kinetics of antigen-antibody reactions at solid-liquid interfaces. J Immunol Methods 1988;113:3–15.
9. Nygren H, Stenberg M. Immunochemistry at interfaces. Immunology 1989;66:321–7.
10. Pugliese, L, Coda A, Malcovati M, Bolognesi M. Three-dimensional structure of the tetragonal crystal form of egg-white avidin in its functional complex with biotin at 2.7 angstrom resolution. J Mol Biol 1993;231:698–710.